ChemComm

COMMUNICATION

Cite this: *Chem. Commun.*, 2015, **51**, 16131

Received 30th August 2015,
Accepted 14th September 2015

DOI: 10.1039/c5cc07277h

www.rsc.org/chemcomm

A highly specific and sensitive electroanalytical strategy for microRNAs based on amplified silver deposition by the synergic TiO_2 photocatalysis and guanine photoreduction using charge-neutral probes†

Rui Li, Shuying Li, Minmin Dong, Liyan Zhang, Yuchun Qiao, Yao Jiang, Wei Qi and Hua Wang*

TiO_2 photocatalysis and guanine photoreduction were synergically combined for amplifying silver deposition for the electroanalysis of short-chain microRNAs with guanine bases using charge-neutral probes. It could allow for the highly specific and sensitive detection of microRNAs in the blood as well as the identification of their mutant levels.

MicroRNAs (miRNAs) are non-coding short-chain RNAs with approximately 18–25 nucleotides in length.[1,2] They are useful diagnostic and prognostic markers for many basic biomedical research studies and evaluations.[3–5] In particular, the expression levels of miRNAs in peripheral blood have been well established to be sensitive biomarkers for cancer diagnostics and metastasis.[3,5] The quantification of free miRNAs in the blood, however, can be challenged by many factors like the short chain length and low expression levels of miRNAs.[6] For example, the common sandwiched detection of short-chain miRNAs of low melting temperature might in a way risk the unwinding of hybridized sequences. Therefore, exploring highly sensitive analysis strategies and suitably efficient detection modes for the analysis of short-chain miRNA targets is of great interest.

In recent decades, many modern analytical methods have been established to quantify or identify miRNA levels, the most known methods being the northern blotting,[7] electrochemical biosensing,[8] reverse transcription polymerase chain reaction,[9] and surface enhanced Raman spectroscopy.[10] Among these classical detection methods, electrochemical biosensing has been recognized as a particularly attractive alternative with high analysis sensitivity, low detection limit, fast response time, cost effectiveness, and ease of automation.[11] For example, Dong and co-workers described a label-free electrochemical biosensor for the detection of miRNAs with the limit of detection down to 67 fM.[12] Gao's group has reported the electrochemical analysis of miRNAs using some special catalyst labels of metal oxides.[8,13,14] A sandwiched electroanalytical protocol has also been developed for the electroanalysis of low-level miRNAs in blood based on silver deposition catalyzed by a gold nanocluster-incorporated enzyme.[1] Noticeably, the catalytic silver deposition procedure has been widely applied as a powerful signal amplification tool;[1,15,16] nevertheless, a common challenge can be mostly encountered regarding the non-specific adsorption of positively charged silver ions onto the oppositely charged phosphodiester backbone probes of nucleic acids. Alternatively, many efforts have been devoted to the use of some nonionic nucleic acid analogs, such as peptide nucleic acids (PNAs)[17] and morpholinos,[18] in the solid-phase assays for nucleic acids. Especially, PNAs with charge-neutral pseudopeptide backbones could serve as outstanding probe candidates for the specific molecular recognition of nucleic acid targets in biosensor design.[19]

Moreover, titanium dioxide (TiO_2), a photocatalyst with excellent chemical stability, low toxicity, low cost, and redox properties, has been extensively applied for solar cells and photocatalytic cleanup of toxic organics in wastewater.[20–22] In 1997, Dunford and colleagues demonstrated that TiO_2 particles could catalyze the DNA damage *in vitro* or in cells.[23] Also, Wamer *et al.* found that guanine, an easily oxidized DNA base, could play a vital role in the photo-oxidative damage of DNA oligonucleotides physisorbed on TiO_2 particles.[24] More importantly, Rajh and co-workers discovered an efficient light-induced crosstalk across the TiO_2 interface and DNA oligonucleotides with guanine bases for the photocatalytic deposition of metallic silver.[25,26]

Inspired by the pioneering work mentioned above, in the present study, a synergic combination of TiO_2 photocatalysis and guanine photoreduction has been proposed for the first time to amplify the silver deposition towards a highly sensitive and selective analysis method tailored for probing guanine-containing miRNAs of hsa-let-7a in blood using charge-neutral PNA probes. Here, the miRNA sequences from the hsa-let-7 family,

Shandong Province Key Laboratory of Life-Organic Analysis, College of Chemistry and Chemical Engineering, Qufu Normal University, Qufu City, Shandong Province 273165, P. R. China. E-mail: huawangqfnu@126.com; Web: http://wang.qfnu.edu.cn; Fax: +86 5374456306; Tel: +86 5374456306

† Electronic supplementary information (ESI) available. See DOI: 10.1039/c5cc07277h

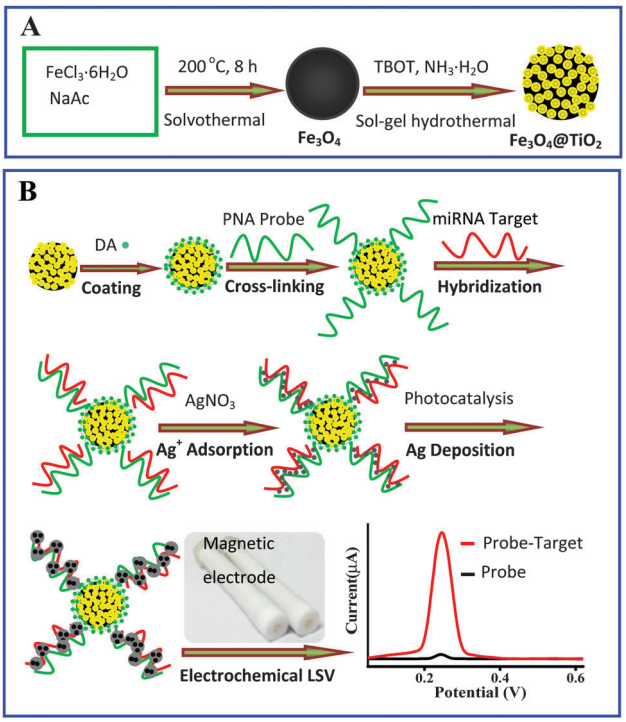

Scheme 1 Schematic illustration of (A) the synthesis procedure of magnetic Fe_3O_4@TiO_2 nanocomposites, for which Fe_3O_4 carriers were prepared *via* the solvothermal method and further shelled by TiO_2 layers through the hydrothermal method, and (B) the main detection procedure and principle for targeting miRNAs containing guanine bases using the Fe_3O_4@TiO_2-DA, including DA coating, PNA probe cross-linking, target miRNA hybridization, Ag^+ adsorption, photocatalytic silver deposition, and electrochemical signal output with magnetic electrodes.

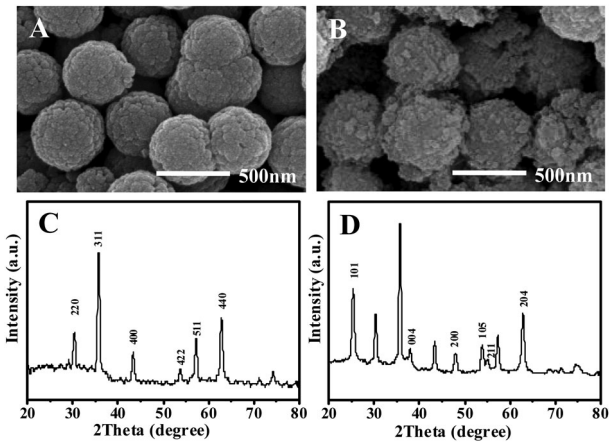

Fig. 1 Representative SEM images of (A) Fe_3O_4 and (B) Fe_3O_4@TiO_2, corresponding to (C) and (D) XRD patterns with the labelled Fe_3O_4 and TiO_2 peaks, respectively.

of which the aberrant expression levels can be associated with the diagnosis and prognosis of cancers. The main detection principle and procedure are schematically illustrated in Scheme 1. As shown in Scheme 1A, magnetic hollow Fe_3O_4 particles were first synthesized using a modified solvothermal method,[27] and then coated with TiO_2 shells by using a modified sol–gel method,[28] resulting in Fe_3O_4@TiO_2 nanocomposites with magnetic separation and photocatalysis functions. Scanning electron microscopy (SEM) imaging was conducted to characterize the resulting Fe_3O_4 particles before and after TiO_2 coating (Fig. 1A). It was found that Fe_3O_4 particles could display a uniformly defined spherical shape with an average size of about 500 nm. Furthermore, as shown in Fig. 1B, TiO_2 layers could be coated onto Fe_3O_4 particles with compact and lumpy structures, and the formed Fe_3O_4@TiO_2 nanocomposites showed an average size of about 570 nm. The crystalline structures of Fe_3O_4 spheres and Fe_3O_4@TiO_2 nanocomposites were further investigated using powder X-ray diffraction (XRD). One can note from Fig. 1C that the marked diffraction peaks of crystalline Fe_3O_4 can be obtained in good agreement with the well established data (JCPDS 75-1609). Importantly, the typical XRD pattern of crystallographic planes marked for anatase-phase TiO_2 could be additionally attained for Fe_3O_4@TiO_2 nanocomposites (Fig. 1D). Moreover, the as-prepared Fe_3O_4@TiO_2 nanocomposites were modified with dopamine (DA) to yield Fe_3O_4@TiO_2-DA. Here, DA as an enediol ligand could be tightly anchored on the nanocrystalline TiO_2 nanoparticles to facilitate their tunable photocatalytic responses in the visible spectral region by adjusting the coordination geometry of Ti atoms on the TiO_2 surface.[29] And the amine group-derivatized Fe_3O_4@TiO_2-DA could be further applied to covalently load the PNA probes for capturing guanine-containing miRNA targets in blood. The main detection procedure and principle are schematically illustrated in Scheme 1B. Herein, miRNA targets containing guanine bases were captured magnetically onto the PNA probe-modified Fe_3O_4@TiO_2-DA. After the introduction of Ag^+ ions, the silver deposition took place by the synergic photocatalysis of TiO_2 on Fe_3O_4@TiO_2-DA and the photoreduction of guanine bases on the targeting miRNAs. The so amplified silver signals were electrochemically measured using the magnetic electrodes for the highly sensitive and selective electroanalysis of guanine-containing miRNAs in blood afterwards.

The analytical performances of silver deposition-based electroanalysis of miRNAs containing guanine bases were comparably investigated, for which the different detection conditions are schematically illustrated (Fig. 2). As shown in Fig. 2A, the electrochemical silver response is much larger in the visible light (Curve a) than in the dark (Curve b), thus confirming that stronger photocatalytic silver deposition could be achieved under the visible light that would be chosen as the necessary condition for the detection of miRNA targets. Furthermore, the silver deposition signal could be neglected for the PNA probes alone, indicating that PNA probes as nonionic nucleic acid analogs could present non-significant adsorption of Ag^+ ions (Curve c). Importantly, it demonstrates that the photcatalytic silver deposition might not occur in the absence of the targeting miRNAs with the photoreducing guanine bases. Moreover, Fig. 2B discloses that Fe_3O_4@TiO_2-DA (Curve a) could exhibit a much greater silver response than Fe_3O_4-DA without TiO_2 (Curve b), indicating that the TiO_2 photocatalyst could play a vital role in the amplified silver deposition.

The Fe_3O_4@TiO_2-DA dosages were optimized for the electrochemical silver responses, showing that 1.0 mg mL^{-1} of

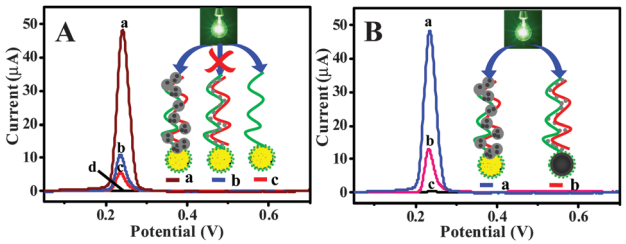

Fig. 2 (A) Comparison of electrochemical responses to wild miRNAs (20 pM) captured by PNA probes-modified Fe_3O_4@TiO_2-DA after the catalytic silver deposition in the (a) presence and (b) absence of visible light, where the responses of the (c) PNA probes-modified Fe_3O_4@TiO_2-DA and (d) blank electrodes were provided as the controls, with the corresponding products schematically illustrated (inset). (B) Electrochemical responses to wild miRNAs (20 pM) captured by the magnetic probes (a) with and (b) without TiO_2 coatings after the photocatalytic silver deposition, taking (c) the blank electrode as the control, with the corresponding detection conditions schematically illustrated (inset).

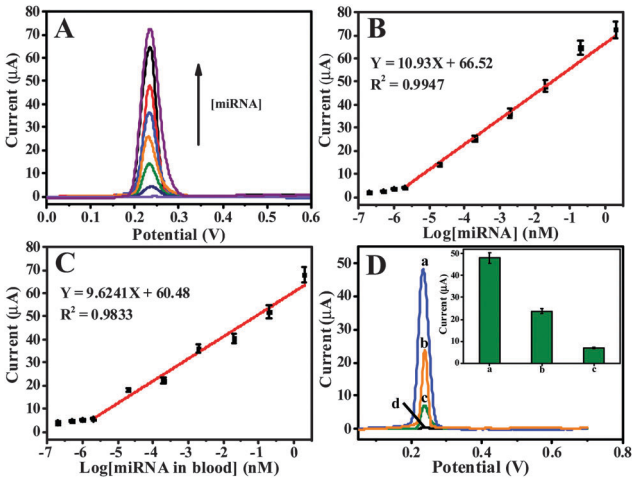

Fig. 3 (A) Electrochemical responses to wild miRNA samples with different concentrations. The calibration curves describing the relationships between the current responses and different logarithmic concentrations of wild miRNA samples spiked in (B) buffer and (C) blood. (D) Comparable investigation of electrochemical responses of the developed electrodes to (a) matched, (b) single-base mismatched, and (c) double-base mismatched miRNAs (20 pM), corresponding to the current changes (inset), where (d) the response to the blank electrode is provided as the control.

Fe_3O_4@TiO_2-DA is enough (Fig. S1A, ESI†). Interestingly, too high concentrations of Fe_3O_4@TiO_2-DA might lead to slightly decreased signals, presumably due to the fact that the non-conductive nanocomposites could be overlaid on the electrode surfaces with too high density so as to conduct the negative effects on the electrochemical silver responses. Also, the influence of the amounts of Ag^+ on the photocatalytic silver deposition was experimentally investigated, showing that the peak currents of silver responses could reach the constant at 1.0 mM $AgNO_3$ (Fig. S1B, ESI†). Furthermore, the time for the probe-target hybridization and photocatalytic sliver deposition reactions was separately explored. As shown in Fig. S1C (ESI†), the electrochemical silver responses could increasingly tend to be steady after 50 min, which was thus chosen as the hybridization reaction time. In addition, Fig. S1D (ESI†) displays that the photocatalytic silver deposition reactions occur very fast, with the saturated silver signals obtained at about 5.0 min.

Under the optimized experimental conditions, the silver deposition-based electroanalytical method was employed to detect the wild and mutated miRNA samples (Fig. 3). Fig. 3A shows the electrochemical responses to wild miRNA targets of different concentrations in buffer. A linear current correlation to the logarithm of the miRNA concentrations was obtained across the concentration range from 2.0 fM to 2.0 nM (R^2 = 0.9947), with the detection limit of 1.3 fM, estimated according to the 3σ rule (Fig. 3B). In the meantime, the developed electroanalytical method was applied to probe the levels of wild miRNAs spiked in blood samples with different concentrations (Fig. 3C). A linear detection relationship between the electrochemical responses and wild miRNA levels in blood was obtained over the miRNA concentrations ranging from 2.0 fM to 2.0 nM (R^2 = 0.9833), with the detection limit of about 1.6 fM. Moreover, the electrochemical responses of the silver deposition to the single-base and double-base mismatched miRNAs were examined by comparing with the wild miRNA targets (Fig. 3D). As expected, the single-base mismatched miRNAs (Curve b) showed much lower responses than the matched ones (Curve a), whereas the double-base mismatched targets could manifest the lowest responses (Curve c), as also illustrated in the inset of Fig. 3D. Accordingly, the as-developed electroanalytical method enables the discrimination of mutation levels of the single-base and double-base mismatched miRNAs. Herein, the mutations of single and double guanine bases of miRNAs might decrease the guanine-enabled photoreduction abilities for silver deposition at different degrees. That is, the photoreduction of guanine bases of miRNAs is highly needed for the photocatalytic silver deposition aforementioned. In addition, the existence of mismatches in the miRNAs might additionally make an insulating barrier to prevent the hole migration to the guanine–guanine accepting sites, leading to a decrease in the TiO_2 photocatalysis for the silver deposition, as also demonstrated elsewhere.[25,26] Therefore, the developed silver deposition-based electroanalysis strategy could allow for the detection of wild miRNA targets in blood with high detection sensitivity and selectivity. Also, it can allow for the quantification of mutant levels of miRNA targets for profiling the RNA expression pattern.

To summarize, in this work, a highly specific and sensitive electroanalytical methodology has been successfully developed for probing guanine-containing miRNA targets in blood based on the amplified silver deposition by the synergic combination of TiO_2 photocatalysis and guanine photoreduction using charge-neutral probes. This silver deposition-based electroanalytical method possesses some outstanding advantages over most of the traditional detection methods for short-chain miRNAs. First, the synergic combination of the photocatalysis of TiO_2 and the photoreduction of guanines of targeting miRNAs could achieve the dramatically amplified signal for silver deposition, which promises a highly sensitive detection of miRNAs specifically containing guanine bases. Second, the coatings of DA on Fe_3O_4@TiO_2 nanocomposites could endow the shelled TiO_2 nanoparticles

with tunable photocatalytic responses in the visible light of great interest, in addition to the covalent loading of captured probes. Third, the use of charge-neutral PNAs might overcome any non-specific adsorption of silver ions to facilitate the highly selective detection of miRNAs. Fourth, the introduction of magnetic carriers could allow for the convenient separation of miRNAs from the complicated blood samples without the tedious purification steps. Finally, the sensitive electrochemical output of silver deposition with magnetic electrodes could facilitate the sensitive detection of miRNAs. Therefore, the developed electroanalytical method could not only probe guanine-containing miRNAs in blood with high sensitivity and selectivity, but also identify their single-base and double-base mutation levels. Importantly, such an electroanalytical mode may be tailored for the short-chain nucleic acids containing reducing guanines. It holds great promise for wide applications in the clinical laboratory for cancer diagnosis and early warning of cancer metastasis.

This work is supported by the National Natural Science Foundation of China (No. 21375075), the Natural Science Foundation of Shandong Province (ZR2014BM025), and the Taishan Scholar Foundation of Shandong Province, P. R. China.

Notes and references

1 Y. M. Si, Z. Z. Sun, N. Zhang, W. Qi, S. Y. Li, L. J. Chen and H. Wang, *Anal. Chem.*, 2014, **86**, 10406–10414.
2 Y. L. Zhou, M. Wang, X. M. Meng, H. S. Yin and S. Y. Ai, *RSC Adv.*, 2012, **2**, 7140–7145.
3 W. C. Cho, *Int. J. Biochem. Cell Biol.*, 2010, **42**, 1273–1281.
4 T. Y. Ha, *Immune Netw.*, 2011, **11**, 11–41.
5 S. M. Hanash, C. S. Baik and O. Kallioniemi, *Nat. Rev. Clin. Oncol.*, 2011, **8**, 142–150.
6 A. W. Wark, H. J. Lee and R. M. Corn, *Angew. Chem., Int. Ed.*, 2008, **47**, 644–652.
7 B. M. Beckmann, A. Grünweller, M. H. W. Weber and R. K. Hartmann, *Nucleic Acids Res.*, 2010, **38**, 147.
8 Z. Q. Gao and Z. C. Yang, *Anal. Chem.*, 2006, **78**, 1470–1477.
9 J. Li, B. Yao, H. Huang, Z. Wang, C. H. Sun, Y. Fan, Q. Chang, S. L. Li, X. Wang and J. Z. Xi, *Anal. Chem.*, 2009, **81**, 5446–5451.
10 J. D. Skell, A. G. Seto, L. P. Jones, S. Jokela, R. A. Dluhy, Y. P. Zhao and R. A. Tripp, *Biosens. Bioelectron.*, 2008, **24**, 923–928.
11 F. Y. Li, J. Peng, Q. Zheng, X. Guo, H. Tang and S. Z. Yao, *Anal. Chem.*, 2015, **87**, 4806–4813.
12 H. F. Dong, S. Jin, H. X. Ju, K. H. Hao, L. P. Xu, H. T. Lu and X. J. Zhang, *Anal. Chem.*, 2012, **84**, 8670–8674.
13 Y. F. Peng and Z. Q. Gao, *Anal. Chem.*, 2011, **83**, 820–827.
14 Y. F. Peng, G. S. Yi and Z. Q. Gao, *Chem. Commun.*, 2010, **46**, 9131–9133.
15 S. I. Stoeva, J. S. Lee, J. E. Smith, S. T. Rosen and C. A. Mirkin, *J. Am. Chem. Soc.*, 2006, **128**, 8378–8379.
16 X. Zhou, S. J. Xia, Z. Q. Lu, Y. Tian, Y. S. Yan and J. Zhu, *J. Am. Chem. Soc.*, 2010, **132**, 6932–6934.
17 J. Weiler, H. Gausepohl, N. Hauser, O. N. Jensen and J. D. Hoheisel, *Nucleic Acids Res.*, 1997, **25**, 2792–2799.
18 N. Tercero, K. Wang, P. Gong and R. Levicky, *J. Am. Chem. Soc.*, 2009, **131**, 4953–4961.
19 J. Zhang, B. P. Ting, N. R. Jana, Z. Q. Gao and J. Y. Ying, *Small*, 2009, **5**, 1414–1417.
20 M. A. Fox, *Top. Curr. Chem.*, 1987, **142**, 71–99.
21 H. Gerischer and A. Heller, *J. Phys. Chem.*, 1991, **95**, 5261–5267.
22 J. M. Rehm, G. L. Mclendon, Y. Nagasawa, K. Yoshihara, J. Moser and M. Grätzel, *J. Phys. Chem.*, 1996, **100**, 9577–9578.
23 R. Dunford, A. Salinaro, L. Z. Cai, N. Serpone, S. Horikoshi, H. Hidaka and J. Knowland, *FEBS Lett.*, 1997, **418**, 87–90.
24 W. G. Wamer, J. J. Yin and R. R. Wei, *Free Radical Biol. Med.*, 1997, **23**, 851–858.
25 J. Q. Liu, L. de la Garza, L. G. Zhang, N. M. Dimitrijevic, X. B. Zuo, D. M. Tiede and T. Rajh, *Chem. Phys.*, 2007, **339**, 154–163.
26 T. Rajh, Z. Saponjic, J. Q. Liu, N. M. Dimitrijevic, N. F. Scherer, M. Vega-Arroyo, P. Zapol, L. A. Curtiss and M. C. Thurnauer, *Nano Lett.*, 2004, **4**, 1017–1023.
27 S. H. Liu, R. M. Xing, F. Lu, R. K. Rana and J. J. Zhu, *J. Phys. Chem. C*, 2009, **113**, 21042–21047.
28 W. F. Ma, Y. Zhang, L. L. Li, L. J. You, P. Zhang, Y. T. Zhang, J. M. Li, M. Yu, J. Guo, H. J. Lu and C. C. Wang, *ACS Nano*, 2012, **6**, 3179–3188.
29 T. Rajh, L. X. Chen, K. Lukas, T. Liu, M. C. Thurnauer and D. M. Tiede, *J. Phys. Chem. B*, 2002, **106**, 10543–10552.

